On The Inclusion of One Double Within CIS and TD-DFT

Vishikh Athavale, Hung-Hsuan Teh, and Joseph Subotnik*

Department of Chemistry, University of Pennsylvania, Philadelphia, Pennsylvania 19104-6323, USA

E-mail: vishikh@sas.upenn.edu,subotnik@sas.upenn.edu

Abstract

We present an improved approach for generating a set of optimized frontier orbitals (HOMO and LUMO) that minimizes the energy of one double configuration. We further benchmark the effect of including such a double within a CIS or TD-DFT configuration interaction Hamiltonian for a set of test cases. We find that, although we cannot achieve quantitative accuracy, the algorithm is quite robust and routinely delivers an enormous qualitative improvement to standard single-reference electronic structure calculations.

1 Introduction

The need for accurate and computationally inexpensive potential energy surfaces has led to the development of a host of electronic structure methods over the last century. In general, accounting for both static and dynamic correlation requires a careful analysis and a delicate methodology as these effects which add together (in one sense) cannot be disentangled[1–3] (in another sense). On the one hand, for chemical processes that involve bond making/breaking,

electronic or energy transfer, static correlation is crucial, as one will strongly mix the ground with a few excited states; the true eigenstates of the Hamiltonian will be combinations of a few nearly degenerate determinants. On the other hand, dynamical correlation describes the weak mixing of one electronic state with many other electronic states; one usually imagines the MP2 energy[4] as a conventional method to recover dynamical correlation correction.

Nowadays, for the most part, if one wishes to account for dynamic correlation, the most common (inexpensive) approach is to use DFT/TDDFT. The successes of DFT are almost uncountable[5,6] even if one must always be hesitant about choosing a functional[7] and overfitting is clearly a problem.[8] And yet, despite the formal foundation of DFT as an exact theory (in principle), in practice there is no question that DFT and TD-DFT do not recover static correlation correctly. For instance, consider the case of conical intersections,[9–11] where two or more electronic states become degenerate. Simulating conical intersections is of great interest given that they are known to mediate many photochemical processes such as internal conversion,[12,13] charge transfer,[14,15] and isomerization.[16] For conical intersections between the ground state (S_0) and the first excited state (S_1), conventional electronic structure methods (including Hartree-Fock (HF)/CIS and DFT/TD-DFT) recover the wrong dimensionality of the seam. More specifically, if a system has N nuclear degrees of freedom, the conical intersection seam should have dimension $N - 2$, but HF/CIS and DFT/TD-DFT theory both predict a seam of dimension $N - 1$ on account of Brillouin's theorem.[17] In the end, it is clear that even if we are prepared to use a DFT Hamiltonian as an approximation to accommodate dynamic correlation, such an ansatz must still be corrected to accommodate static correlation. In other words, to treat problems with bond-making/breaking, we require a DFT/TD-DFT ansatz with a more balanced treatment of ground state and excited states.

Now, even if we are prepared to use the DFT Fock operator and the TD-DFT linear response operator as matrix elements of a large configuration interaction Hamiltonian, there are many possibilities for including static correlation. For instance, within a wave function picture, static correlation is most easily treated with multi-reference methods whereby one

optimizes the energy of one many-body state (or a collection of many-body states) by both diagonalizing a large matrix and optimizing orbitals at the same time. To that end, Gagliardi et al. [18,19] have proposed multiconfigurational pair-DFT where a reference wave function of multiconfigurational nature is used for obtaining the static component of the total energy, which is then combined with the energy from a density functional for the calculation of the remainder of the total energy (i.e. the dynamic correlation energy). Semiempirical DFT-MRCI methods were proposed by Grimme and Waletzke [20] and allow calculation of excited states of large molecules. [21] Recently, quite a few methods have been proposed to rectify the specific failure of DFT/TDDFT [22–25] so as to recover static correlation and the correct topology of a conical intersection, while retaining the fundamental density functional formulation. For example, Truhlar *et al* proposed introducing a non-zero coupling between the DFT ground state and single-excitation TD-DFT response states by artificially using two different functionals within a DFT/TDA calculation (the so-called DF-TDA [26] and CIC-TDA [27] methods). Spin flip DFT methods [28,29] that start from a high-spin triplet state as a reference and produce the ground and excited states using a spin-flip excitation operator have shown strong success in describing conical intersections. [30,31] Through the route presented by constrained DFT [32] one can calculate diabatic representations and excitation energies in the vicinity of conical intersections. [33] Recently, Mei and Yang [34] have put forth the QE-DFT method that calculates excited state energies starting from a system deficient by one electron. This list is not exhaustive. [35,36] In short, there are many approaches today that seek to achieve a more balanced treatment of static and dynamic correlation effects within a DFT/TD-DFT framework.

From our perspective, unfortunately, many of the methods above are not ideal for running nonadiabatic dynamics. In particular, because some of these methods require a predetermined set of orbitals in the active space, dynamics using such methods are prone to user error if the user chooses the wrong set of orbitals (and this error is not corrected until after a long simulation). Moreover, whenever one chooses a set of active orbitals, there is

no guarantee that one can generate a smooth set of orbitals (and therefore energies) as a function of nuclear geometry; it is well known that CASSCF potential energy surfaces can have strange discontinuities.[37–39] In the end, the ideal merger of DFT theory with static correlation theory would occur in a black box fashion, such that the user need not choose orbitals, the relevant potential energy surfaces are smooth (or as smooth as possible), and the relevant active space should include the standard DFT ground state.

With this goal in mind, recently we introduced the CIS-1D and TDDFT-1D method[40] inspired by the idea of calculating states of double excitation character in linear response TD-DFT by Maitra et al.[41] The CIS-1D method works as a configuration interaction method whose Hamiltonian has a basis of the following states: the Hartree-Fock (HF) ground state $|\psi_0\rangle$, the set of singly excited states $|\psi_i^a\rangle$ as in a CIS Hamiltonian, and finally one optimized doubly excited state $\left|\psi_{h\bar{h}}^{l\bar{l}}\right\rangle$, where a pair of electrons are excited from an orbital $|h\rangle$ to $|l\rangle$. As a matter of notation, throughout this manuscript $\{i, j, k, \ldots\}$ denote occupied orbitals, $\{a, b, c, \ldots\}$ denote virtual orbitals, and $\{p, q, r, \ldots\}$ denote general orbitals. The configuration interaction Hamiltonian in CIS-1D is

$$
\mathbf{H} = \begin{pmatrix}
\epsilon_{HF} & 0 & \langle\psi_0|H|\psi_{h\bar{h}}^{l\bar{l}}\rangle \\
0 & \langle\psi_i^a|H|\psi_j^b\rangle & \langle\psi_i^a|H|\psi_{h\bar{h}}^{l\bar{l}}\rangle \\
\langle\psi_0|H|\psi_{h\bar{h}}^{l\bar{l}}\rangle & \langle\psi_{h\bar{h}}^{l\bar{l}}|H|\psi_i^a\rangle & \langle\psi_{h\bar{h}}^{l\bar{l}}|H|\psi_{h\bar{h}}^{l\bar{l}}\rangle
\end{pmatrix}. \tag{1}
$$

Within the Tamm-Dancoff Approximation (TDA),[42,43] one can construct a configuration interaction Hamiltonian built on top of a set of Kohn-Sham (KS) reference orbitals in direct analogy to the CIS methodology. This gives rise to the TDDFT-1D method. For this ansatz, in Ref. 40, using stilbene as an example, we showed that smooth potential energies can be obtained along the torsional coordinate along the double bond, especially around the avoided crossing (where TD-DFT fails). Furthermore, for the conical intersection between the S_0 and S_1 state of the water molecule, TDDFT-1D recovered the correct topology as well.

Despite the aforementioned successes, over the past few months, we have run TD-DFT-1D and CIS-1D calculations for a host of molecules and found that the algorithm presented in Ref. 40 for finding the optimal double excited state does not always converge, and the results were not necessarily stable. To that end, the objectives of this manuscript are twofold. First, we will present a new, robust algorithm for calculating the minimum energy doubly excited state that is nearly guaranteed to converge (and thus isolate the correct optimized HOMO and LUMO). Second, we will benchmark the CIS-1D/TD-DFT-1D approach on a set of representative examples where one will quickly be able to assess the relative strengths and weaknesses of the ansatz. Overall, our finding is that though the method is not quantitatively accurate, the inclusion of a single double can offer an outstanding, qualitative correction to single-reference methods like DFT.

2   Theory

The TDDFT-1D method hinges on selecting one doubly excited state to account for electron correlation. We choose this doubly excited state to be the excitation of a pair of electrons from the HOMO $|h\rangle$ to the LUMO $|l\rangle$. In doing so we seek the optimal $|h\rangle$ and $|l\rangle$ orbitals, chosen from the occupied and the virtual space respectively, that minimize the energy for the double excitation. This doubly excited state is denoted as $\left|\psi_{h\bar{h}}^{l\bar{l}}\right\rangle$. In Ref. 40, the optimized $|h\rangle$ and $|l\rangle$ orbitals were isolated by self-consistently finding occupied-occupied and virtual-virtual unitary matrices that independently rotated the occupied and virtual subspaces so as to minimize the energy of the double excitation $E_d(= \langle\psi_{h\bar{h}}^{l\bar{l}}|H|\psi_{h\bar{h}}^{l\bar{l}}\rangle)$. While we won't repeat the procedure here, it is important to emphasize that the minimization procedure effectively used information from the first derivative of the E_d (as differentiated with respect to orbital rotations). Unfortunately, after applying the procedure in Ref. 40 for bigger molecules, we have found that the method has shortcomings (see Section 4 below). To that end, we will now present an improved algorithm for computing optimized orbitals which is based on a

5

Newton-Raphson optimization technique.

The energy of the doubly excited state E_d is a function of the "inactive" (non-frontier) orbitals as well as the $|h\rangle$ and $|l\rangle$ orbitals. Starting from an HF reference state, it is straight-forward to show that

$$E_d = \langle \psi_{h\bar{h}}^{l\bar{l}}|H|\psi_{h\bar{h}}^{l\bar{l}}\rangle = E_0 - 2f_{hh} + 2f_{ll} + (hh|hh) + (ll|ll) + 2(hl|lh) - 4(hh|ll). \quad (2)$$

Here, f_{pq} are the elements of the Fock matrix, and terms of the form $(pq|rs)$ stand for two-electron integrals in the chemist's notation. E_0 is the ground state energy. Within CIS-1D/TDDFT-1D, the optimized orbitals $|h\rangle$ and $|l\rangle$ are generated from independent rotations of the orbitals in the occupied and virtual spaces, respectively. We emphasize that such rotations keep the energy of the ground state unchanged, and so one can effectively consider E_d to be a function of $|h\rangle$ and $|l\rangle$ only. Thus, if the relevant rotation matrices have the form e^{Θ} (where Θ is an anti-symmetric matrix), we must compute only the optimized HOMO and the LUMO so that the Θ matrix takes the following simple form:

$$\Theta = \left(\begin{array}{cccc|cccc}
0 & \cdots & 0 & \theta_{1h} & & & & \\
0 & \cdots & 0 & \theta_{2h} & & & & \\
\vdots & \ddots & & \vdots & & & \mathbf{0} & \\
0 & \cdots & 0 & \theta_{h-1,h} & & & & \\
-\theta_{1h} & \cdots & -\theta_{h-1,1} & 0 & & & & \\
\hline
& & & & 0 & -\theta_{l+1,l} & \cdots & -\theta_{ln} \\
& & & & \theta_{l+1,l} & 0 & \cdots & 0 \\
& \mathbf{0} & & & \vdots & \vdots & \ddots & \\
& & & & \theta_{nl} & 0 & \cdots & 0
\end{array}\right). \quad (3)$$

For infinitesimally small rotations, the orbitals $|h\rangle$ and $|l\rangle$ after rotation are

$$\left|\tilde{h}\right\rangle = |h\rangle - \sum_i \theta_{ih} |i\rangle - \sum_i \frac{\theta_{ih}^2}{2} |h\rangle, \tag{4a}$$

$$\left|\tilde{l}\right\rangle = |l\rangle - \sum_a \theta_{al} |i\rangle - \sum_a \frac{\theta_{al}^2}{2} |l\rangle. \tag{4b}$$

Using these so-called "exponential" coordinates, E_d (which is now a function of $\left|\tilde{h}\right\rangle$ and $\left|\tilde{l}\right\rangle$) can be written as a function of $\{\theta_{ih}\}$ and $\{\theta_{al}\}$. We will now apply the Newton-Raphson optimization as a function of the variables $\{\{\theta_{ih}\}, \{\theta_{al}\}\}$. According to such an approach, we will take steps in Θ that are informed from the gradient and Hessian of E_d. These quantities are given by

$$\frac{\partial E_d}{\partial \theta_{ih}} = 4 \left(f_{ih} - (ih|hh) + 2(ih|ll) - (il|lh) \right) \tag{5a}$$

$$\frac{\partial^2 E_d}{\partial \theta_{ih} \partial \theta_{jh}} = 4\delta_{ij} \left(f_{hh} - (hh|hh) + 2(hh|ll) - (hl|lh) \right)$$

$$- 4 \left(f_{ij} - 2(hi|hj) + (hh|ij) + 2(ij|ll) - (il|lj) \right) \tag{5b}$$

$$\frac{\partial E_d}{\partial \theta_{al}} = 4 \left(f_{al} - (al|ll) + 2(al|hh) - (ah|hl) \right) \tag{5c}$$

$$\frac{\partial^2 E_d}{\partial \theta_{al} \partial \theta_{bl}} = -4\delta_{ab} \left(f_{ll} - (ll|ll) + 2(hh|ll) - (hl|lh) \right)$$

$$+ 4 \left(f_{ab} - 2(hh|ab) + (hb|ah) + 2(la|bl) - (ll|ab) \right) \tag{5d}$$

$$\frac{\partial^2 E_d}{\partial \theta_{al} \partial \theta_{ih}} = 4(ia|lh) + 4(il|ah) - 16(ih|al). \tag{5e}$$

We may now summarize our algorithm for computing the optimized frontier molecular orbitals:

1. Solve the self-consistent field equations to obtain the cannonical HF molecular orbital (MO) coefficient matrix $\mathbf{C}$.

2. Calculate the gradient vector $\mathbf{g} = \begin{pmatrix} \frac{\partial E_d}{\partial \theta_{ih}} \\ \frac{\partial E_d}{\partial \theta_{al}} \end{pmatrix}$ and the Hessian $\mathcal{H}$.

3. Solve for θ_{ih} and θ_{al} using the equation $\mathcal{H}\theta = -\mathbf{g}$. Here $\theta = \begin{pmatrix} \theta_{ih} \\ \theta_{al} \end{pmatrix}$.

4. Construct the $\boldsymbol{\Theta}$ matrix as described in eq 3.

5. Obtain the new MO coefficients $\tilde{\mathbf{C}} = \mathbf{C}e^{\boldsymbol{\Theta}}$.

6. If $|\tilde{\mathbf{C}} - \mathbf{C}|$ is below a threshold then the optimization has converged. Else go to setp 2 with $\mathbf{C} = \tilde{\mathbf{C}}$.

Note that, for the algorithm above, the Hessian is only of size $N - 2$, where N is the size of the atomic basis. For the most part, inversion of $\mathcal{H}$ carries minimal cost.

Extending the method above to work with TDDFT-1D is also straightforward. One works with the KS orbitals as if they were real orbitals and one defines a key double excitation of the KS ground state wave function from the HOMO to the LUMO. The energy of this doubly excited state is

$$E_d = E[\rho_d] = 2\sum_i{}' h_{ii} + 2\sum_{ij}{}'(ii|jj) - c_{HF}(ij|ji) + (1 - c_{HF})E_{xc}[\rho_d] \tag{6}$$

The electron density obtained by exciting a pair of electrons from orbital $|h\rangle$ to $|l\rangle$ is denoted by ρ_d. h_{ii} refers to the one-electron interaction terms. The summation in the expression is primed to indicate that the summation is over the orbitals $1, 2, \ldots, h - 1, l$ (orbital $|h\rangle$ is omitted and $|l\rangle$ is included). For a hybrid xc functional c_{HF} is the factor of the Hartree-Fock exchange. $E_{xc}[\rho]$ is the xc energy functional for a given density ρ. Just as for the CIS-1D case, in order to find the optimized doubly excited state we rotate the KS orbitals using a rotation operator of the form $e^{\boldsymbol{\Theta}}$. As compared with the expressions for the gradient and Hessian above (Eq. 5), besides the factor of c_{HF}, the gradient and Hessian have the following

additional terms from differentiating the xc functional:

$$\frac{\partial E_{xc}[\rho_d]}{\partial \theta_{ih}} = \int \phi_i(\mathbf{r}) \left.\frac{\partial E_{xc}}{\partial \rho(\mathbf{r})}\right|_{\rho=\rho_d} \phi_h(\mathbf{r}) \mathrm{d}\mathbf{r} \tag{7}$$

$$\frac{\partial^2 E_{xc}[\rho_d]}{\partial \theta_{ih} \partial \theta_{jh}} = \int \phi_h(\mathbf{r}) \phi_i(\mathbf{r}) \left.\frac{\partial^2 E_{xc}}{\partial \rho(\mathbf{r}) \partial \rho(\mathbf{r}')}\right|_{\rho=\rho_d} \phi_h(\mathbf{r}') \phi_j(\mathbf{r}') \mathrm{d}\mathbf{r} \mathrm{d}\mathbf{r}'. \tag{8}$$

3   Results

We have implemented the schemes above so as to apply the CIS-1D and the TDDFT-1D formalisms to reasonably sized molecules. We will now discuss our findings.

3.1   PYCM

Our first example is the molecule 2-(4-(propan-2-ylidene)- cyclohexylidene)malononitril), or PYCM. PYCM is a donor-acceptor molecule that possesses two low-lying excited states, one of which is of charge transfer (CT) character and the other one has local excitation character.[44] Its photoemission spectrum indicates that the CT state fluoresces whereas the non-CT state undergoes a radiationless decay. The twisting of the double bond between the cyclohexane ring and the cyano groups purportedly gives rise to an avoided crossing between the S_1 and S_2 states, which mediates photochemical processes. Previous work has analyzed the S_2/S_1 crossing at angles $\sim 40°$[45] but has not directly addressed a potential crossing at 90° when the molecule fully distorts (and the double bond breaks). Presumably, one can expect that twisting PYCM should behave something like twisting ethylene.

In Fig. 1, we present the potential energy curves of PYCM starting from its ground state minimum geometry and following along the torsional angle of the double bond. We evaluate the performance of the TDDFT-1D/B3LYP method against that of the TDA/B3LYP using a basis set of 6-31G*. For the TDDFT-1D calculation, the key doubly excited state is easily found using the algorithm described above in Sec. 2; convergence details will be provided in Sec. 4 below. The TDDFT-1D calculation yields smooth curves that will allow nonadiabatic

simulations of the photodynamics of this molecule (with at least qualitative accuracy, on par with usual TD-DFT excited-state calculations).

Lastly, in Fig. 1, we also plot the dipole moments of the individual excited states. Here, one can learn a great deal about the nature of photo-chemistry for the present system. Note that there is a true crossing between S_2 and S_1–the dipole moments of these states switch character around 62°. However, there is no such crossing between the dipole moments of S_1 and S_0. Moreover, although not plotted here, we find that a variety of diabatization schemes (including Boys,[46] etc.) do not predict a meaningful diabatic crossing according to this degree of freedom–which has clear consequences for nonadiabatic dynamics. Presumably, as for the case of ethylene,[47] there will be a conical intersection between S_0 and S_1 at some distorted geometry, but we cannot yet isolate such a geometry without gradients.
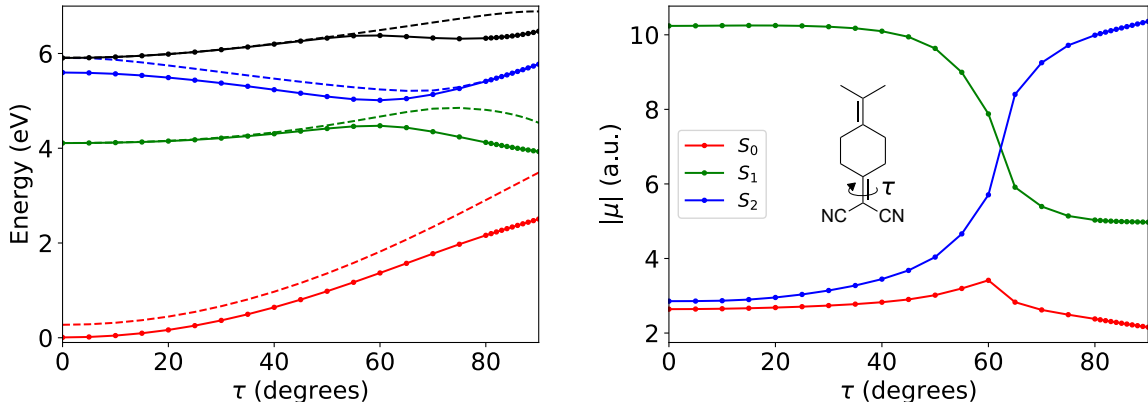

Figure 1: Potential energy curves for the PYCM molecule (left) and diploe moments $|\mu|$ (right) along the torsional angle τ. On the left, the S_0, S_1, S_2, S_3 energies for TDDFT-1D B3LYP/6-31G* are plotted using solid lines in red, green, blue and black respectively. The dashed lines represent the energies for the same states calculated using B3LYP/TDA. The dipole moments of the TDDFT-1D states S_1 and S_2 cross around 62°. The torsional angle τ is represented in the inset in the plot on the right. Note that there is no avoided crossing between $S_0 - S_1$ states at 90° according to an analysis of their dipole moments.

3.2 Thiophene

Our next example is the thiophene molecule whose oligomers have drawn attention as materials useful for energy conversion technology.[48–50] The photo-decay for a standard thiophene molecule is dominated by internal conversion through a conical intersection, whereas higher chain oligothiophenes show a significant rate of intersystem crossing (ISC).[51] The photo-deactivation pathway for bithiophene (occurring through ISC as well as through S_0/S_1 conical intersection) was investigated in Ref 51 using EOM-CCSD. Here we investigate the potential energy curves of bithiophene using the TDDFT-1D method. For this molecule, an optimized ground state geometry at the B3LYP/6-311G** level was reported in Ref. 51. Furthermore, there are two S_1 minimum structures at the CASSCF/6-31G* level, S_1-min-a and S_1-min-b, which are closed- and open-ring structures respectively. There are some low-lying conical intersection geometries between S_0 and S_1 identified at the CASSCF level in Ref. 51.

In Fig. 3, potential energy curves are plotted along a linear interpolation coordinate starting from the S_0 minimum structure to the S_1-min-a, and continuing on to the open ring S_1-min-b. In Fig. 3a, we plot data for DFT/TDA and in 3b we plot data for TD-DFT-1D. The vertical excitation energies to S_1 at the Franck Condon point for the B3LYP/TDA, TDDFT-1D and CASPT2 methods are 4.36 eV, 4.40 eV, and 4.51 eV[51] respectively. These energies agree reasonably well with the experimental value of 4.24 eV[52] (from an absorption spectrum at room temperature for the molecule in the gas phase).

According to Fig. 3, both B3LYP/TDA and TD-DFT-1D predict a S_0/S_1 crossing as we interpolate between S_1-min-a and S_1-min-b. However, for the B3LYP/TDA, this crossing is unphysical: because we employ a restricted DFT calculation, the S_1 (TDA) energy drops below the S_0 (DFT) energy around $\xi = 1.9$, corresponding to a negative excitation energy. In Fig. 4, we zoom in on this spurious behavior. Note that for such TD-DFT/DFT crossings, it is well known that the topology of an S_0/S_1 crossing is incorrect; the branching plane has the wrong dimensionality[17] (whether or not we use a restricted or unrestricted KS scheme).

Finally, note that all of these incorrect features are fixed up (at least qualitatively) using the TDDFT-1D calculation; for the present case, including one double introduces a small S_1-S_0 gap and presumably shifts the location of the conical intersection slightly. The TD-DFT-1D potential energy curves compare reasonably well with the EOM-CCSD surfaces reported in Ref. 51.
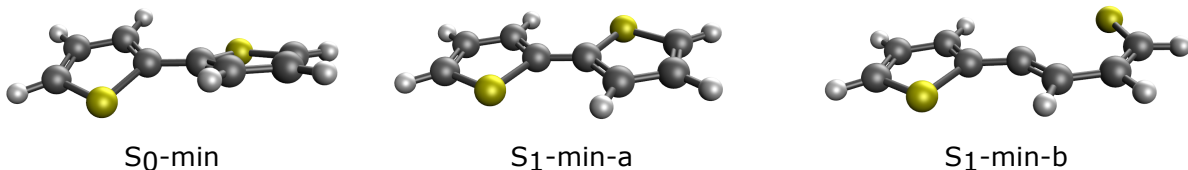

Figure 2: The structures of the optimized bithiophene molecule from Ref 51. The S_0 minimum geometry is calculated using B3LYP/6-311G** and the two S_1 minima, S_1-min-a and S_1-min-b, are calculated using CASSCF/6-31G*.
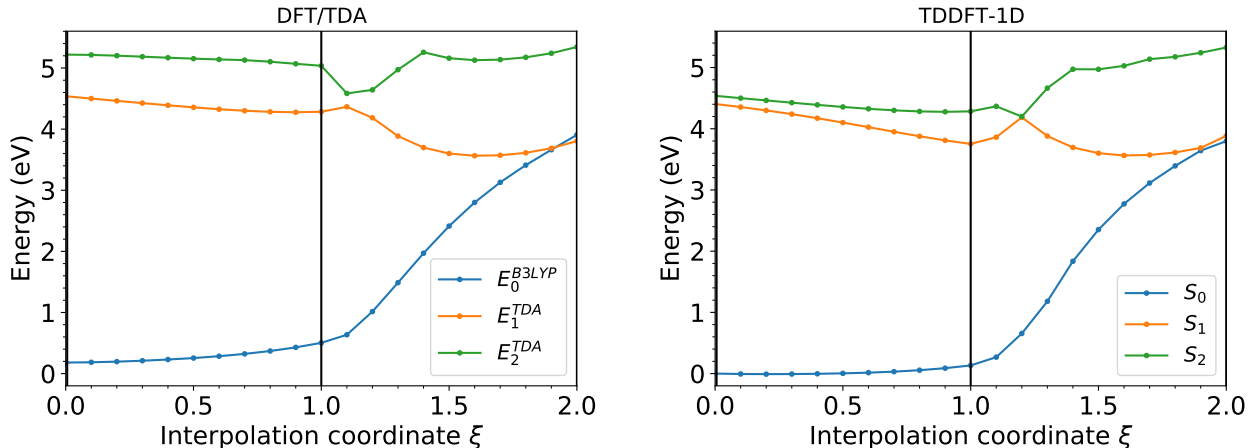

Figure 3: Potential energy curve of the S_0, S_1 and S_2 states of the bithiophene molecule along the linear interpolation coordinate ξ calulated using B3LYP/TDA (left) and TDDFT-1D (right). Here $\xi = 0$ corresponds to the the S_0 minimum geometry, $\xi = 1$ corresponds to the S_1-min-a geometry, and $\xi = 2$ to the S_1-min-b geometry.

3.3 LiF

Our last example is the dissociation curve of the LiF molecule, for which restricted Hartree-Fock (RHF) solution is known to be inadequate as far as dissociating into neutral Li and F fragments is concerned. The ground state RHF curve leaves the Li and F atoms in a closed
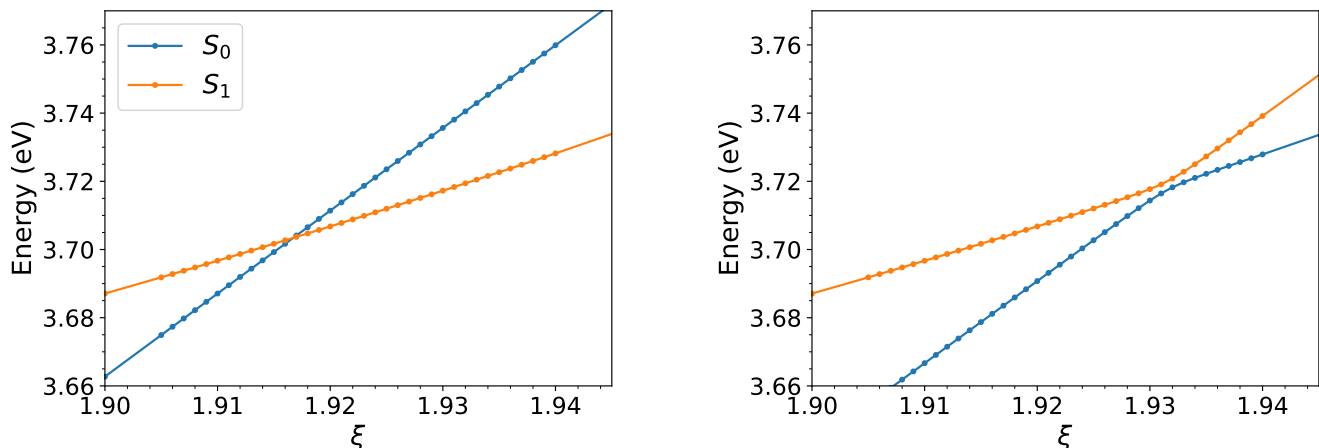
Figure 4: A zoom in on the S_0/S_1 potential energy curves plotted in Fig 3. The B3LYP/TDA calculation (left) predicts a spurious crossing of the S_0/S_1 states. This behavior is corrected in the TDDFT-1D calculation, and a small gap is introduced between the S_0 and S_1 states.

shell state with some ionic character; this state becomes degenerate with the first excited CIS state as LiF dissociates. Although LiF is reasonably small, LiF represents a difficult case for CIS-1D/TD-DFT-1D calculations because, at long distances, the true ground state is very different from the RHF solution; dissociating LiF is not like twisting the double bond of PYCM, whereby the doubles correction is important only at various intermediate angles (close to 90°).

In Fig. 5a, we plot RHF vs CIS-1D potential energy curves. We find that, by including one double only, the CIS-1D method is able to substantially correct for the static correlation errors and dissociate the molecule. We plot the ground state S_0 and first excited state S_1 energy curves. Admittedly, the CIS-1D ground state curve is not completely size-consistent;[40] the S_0 curve does not reach the sum of the individual Li and F energies (here, energy 0) when the molecule dissociates. Nevertheless, qualitatively, the behavior of the S_0 and S_1 states is correct and far improved over RHF. Although not plotted here, note that while the spin contaminated unrestricted Hartree-Fock (UHF) solution does recover the correct zero energy dissociation limit (i.e. the method is size-consistent), as is well known, the UHF S_0 curve shows a kink[53] at the point where RHF and UHF solutions diverge. Furthermore,
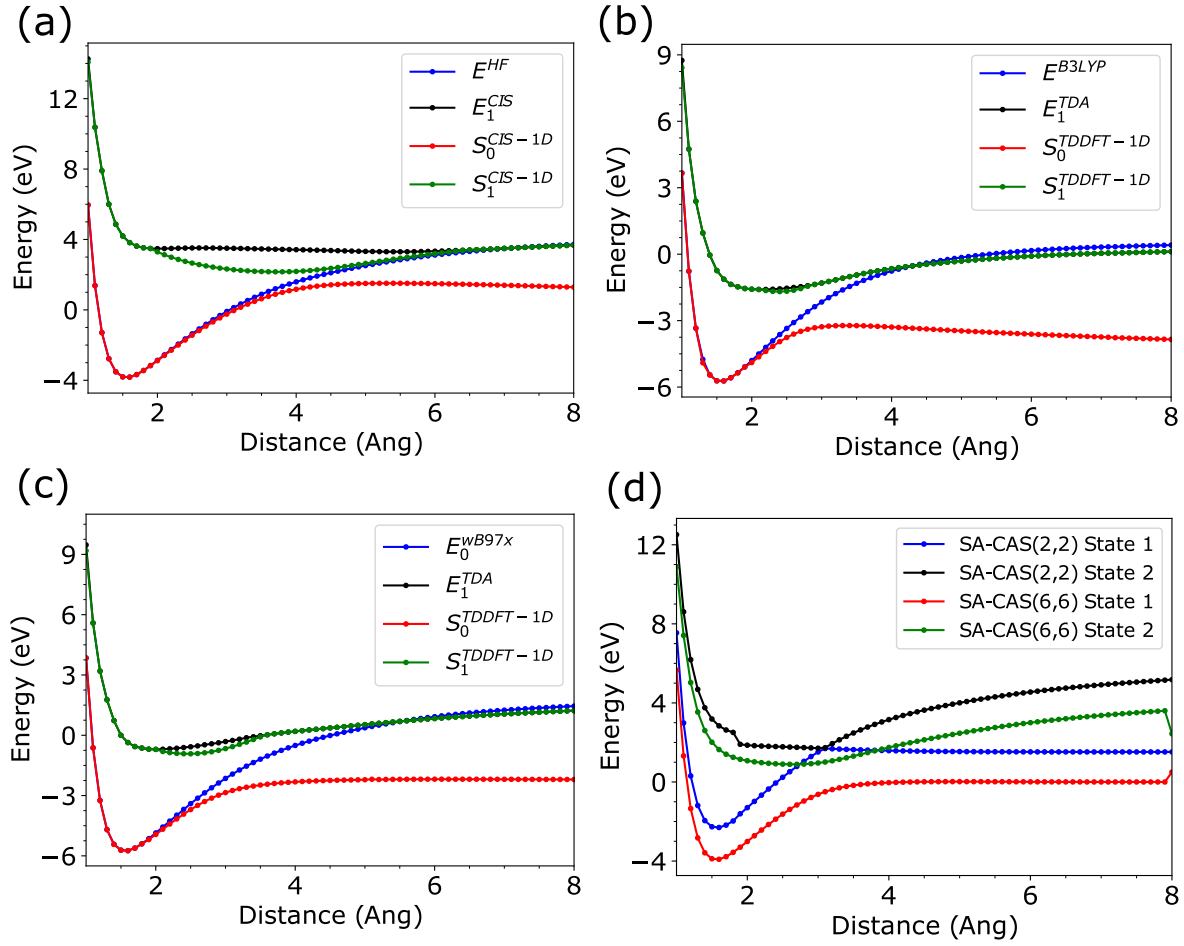
Figure 5: Potential energy curves of the lowest two singlet states for the dissociation of LiF molecule calculated using (a) RHF/CIS and CIS-1D, (b) B3LYP/TDA and TDDFT-1D, (c) ωB97X/TDA and TDDFT-1D, and (d) SA(2)-CASSCF(2,2) and SA(2)-CASSCF(6,6). All the calculations were performed using the 6-31G* basis set.

UCIS energies computed on top of a UHF reference are wildly discontinuous. By contrast, the CIS-1D solution is spin-pure, smoother, and at least qualitatively correct.

Next, in Fig. 5b, a calculation of B3LYP/TDDFT-1D is compared with that of B3LYP/TDA. The restricted KS method is unable to dissociate the molecule correctly and actually shows an unphysical crossing with the TDA state around 4.3 Å. By contrast, according to TDDFT-1D, the ground state S_0 and excited state S_1 solutions are well separated. Note, however, that when we employ the B3LYP ground state reference, TD-DFT-1D predicts (incorrectly) an artificial barrier in the dissociation curve. One must wonder whether such an artifact arises from the familiar problem of DFT self-interaction error,[54] which can severely limit the ability of standard DFT to dissociate bonds. To test such a hypothesis, in Fig. 5c, we plot potential energy surfaces using the ωB97X[55] functional, which is a long-range corrected functional with minimal self-interaction energy (at least at long range). Note that, if we use a range-corrected restricted KS wave function, the S_0 curve becomes flat as the molecule dissociates and yields the correct physics (at least qualitatively). Clearly, the take-home message is that including one double can capture a good amount of correlation and fix many problems in DFT but at the same time, one is still strongly limited by the choice of an approximate exchange-correlation functional.

Lastly, let us address the nature of the CIS-1D solution and its relationship to more established multi-reference methods. CIS-1D does not optimize the ground state orbitals, but rather builds a configuration interaction Hamiltonian by including all single excitations and one (optimized) double excitation. A more standard approach is to optimize the orbitals for an active space in a self-consistent manner, i.e. CASSCF. One might wonder how CIS-1D compares with CASSCF method. In Fig. 5d, we plot the results for SA(2)-CASSCF(2,2) and SA(2)-CASSCF(6,6) methods performed using OpenMolcas.[56] In the (2e,2o) active space no symmetry was considered. For the (6e,6o) calculation the C_{2v} symmetry was enforced and the active space had 2 orbitals each of symmetry species a_1, b_1, and b_2. We find that SA-CASSCF(2,2) produces potential energy surfaces with strange discontinuities. In the calcula-

tion with larger active space the correct physics is recovered qualitatively but discontinuities still exist. As far as energetics are concerned, high-level quantum chemical calculations[57] as well as experiments[58] show that the bond dissociation energy is about $6.0\,\mathrm{eV}$, which is clearly underestimated by all calculations. Admittedly our calculations were not at the complete basis set limit.
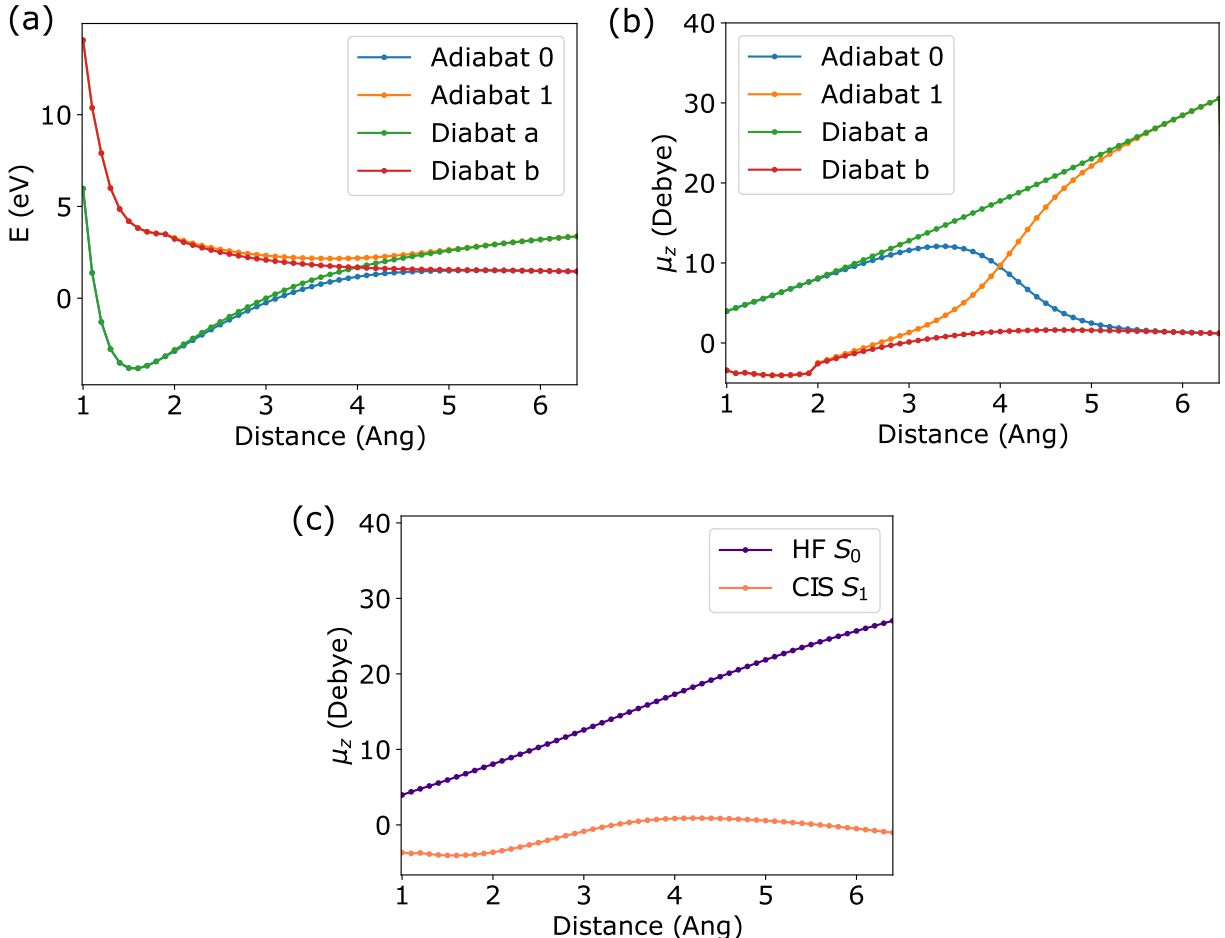

Figure 6: (a)CIS-1D Energy E and (b) dipole moments for the lowest two adiabatic states (the S_0 and S_1 states) and diabatic states for LiF. In (c) the dipole moment of the lowest two adabatic states from RHF/CIS calculation is plotted as a function of LiF bond distance. Note that while the CIS-1D adiabats show a crossing in their dipole moment (indicating a change in their charge character), the RHF/CIS adiabats do not cross, and predict the wrong charge character as LiF dissociates.

Finally, one of the biggest advantages of a multireference method is the capacity to generate diabatic states for S_0/S_1 crossings. Since CIS-1D has some multi-reference character

– e.g., the states produced from CIS-1D (TDDFT-1D) are a linear combinations of the reference HF (KS) wave function, the CIS (TDA) states, and one doubly excited state – one would hope that CIS-1D can produce meaningful diabats. After all, the method produces ground and excited states on a reasonably equal footing. This state of affairs stands in contrast to any diabatization scheme based on mixing the HF ground state and CIS states. In the latter case, one expects that all results will be far less meaningful on account of Brillouin's theorem such that, e.g., there is no guarantee of smooth diabatic surfaces.

In Fig. 6, we plot CIS-1D diabats as produced using the Boys localization method.[46] Applying Boys diabatization to CIS-1D (TDDFT-1D) states is fairly straightforward and requires only the dipole moment matrix elements, which are calculated explicitly in the Appendix. In Fig. 6a, we plot the two lowest CIS-1D adiabatic and diabatic energies for the LiF molecule; in Fig. 6b, we plot the relevant dipole moments in the avoided crossing region. Clearly, CIS-1D is able to reproduce smooth, qualitatively correct diabatic states. The dipole moment of the CIS-1D ground state is ionic at equilibrium bond distances but correctly vanishes as the LiF molecule dissociates into neutral fragments. The CIS-1D diabatic states have fixed charge character and correctly interpolate between the S_0 and S_1. Note that the RHF and CIS dipole moments, plotted in Fig. 6c, are (of course) completely invalid.

4 Discussion

The data above has demonstrated that, when converged, TD-DFT-1D can predict a large qualitative change in practical electronic structure calculations by including one double configuration. Having found such a result, let us now show how convergence can be difficult and why the present algorithm is necessary. In Fig. 7, we demonstrate that the previous minimization algorithm (described in Ref. 40) fails to converge for the PYCM molecule. In particular, note that Newton-Raphson minimization converges in 8 iterations, while the old method at first *increases in energy* and eventually simply oscillates back and forth along the

incorrect asymptote. We have also found that the algorithm in Ref. 40 can fail to converge to the correct set of orbitals for certain LiF geometries. In general, by coordinating the occ-occ and virt-virt rotations through the Hessian $\mathcal{H}$, the Newton-Raphson method is clearly quite a few steps ahead with regards to the stability of optimization.
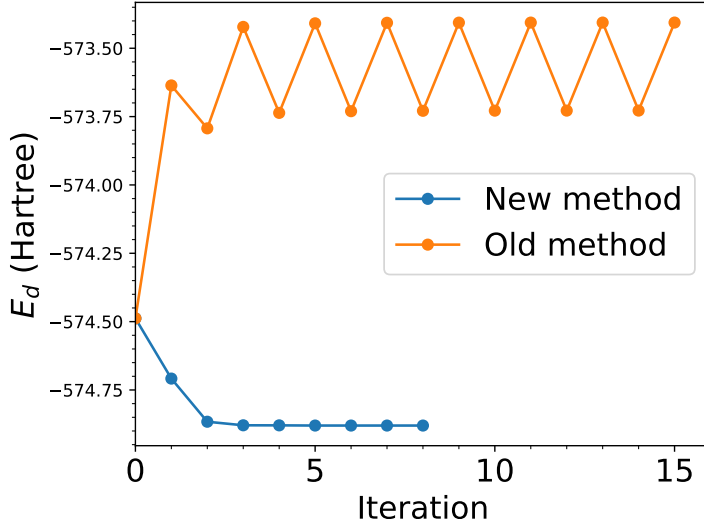

Figure 7: Energy of the doubly excited state E_d at each iteration step of the minimization process for PYCM molecule at $\tau = 40°$. The old method of minimization in Ref 40 is unable to find the optimized frontier orbitals as E_d oscillates around a value that is higher than that obtained from the initial set of orbitals. In contrast, the new method outlined in this manuscript finds a solution that converges fairly quickly to the correct minimum.

At this point, the key item remaining is the question of efficiency and computational time: how expensive is it to construct the orbital Hessian above in Sec. 2? To answer this question, at the moment it is essential to distinguish between CIS-1D and TD-DFT-1D. First, we address CIS-1D. For the present implementation, the cost of the algorithm comes out to be 1.3 s CPU time per iteration (for the case of the PYCM molecule), whereas the algorithm in Ref. 40 takes 0.3 s per iteration for the same molecule – but note that the latter algorithm never converges. Overall, the algorithm from Ref. 40 requires the diagonalization of two matrices (one of size $N_o \times N_o$, another of size $N_v \times N_v$). By contrast, the present algorithm requires the inversion of one matrix (of size $N \times N$). Here, N_o is the number

18

of occupied orbitals, N_v is the number of virtual orbitals, and $N = N_o + N_v$ is the total basis size. Thus, the present algorithm should be some constant factor more expensive than the previous algorithm (per iterative step). Note that the present algorithm also requires computing three sets of density matrix times electron repulsion integrals (so-called J/K subroutines), whereas the previous algorithm required only one such call. In the end, one might expect that, per iteration, the present algorithm will be three times as expensive as the previous approach – though requiring far fewer iterations and also converging in a far more robust fashion.

Next, we turn to TD-DFT-1D, for which the bottleneck for the minimization algorithm is the calculation of the matrix elements of the exchange-correlation kernel in the adiabatic approximation $f^{xc}(\mathbf{r}, \mathbf{r}') = \frac{\partial^2 E_{xc}}{\partial \rho(\mathbf{r}) \partial \rho(\mathbf{r}')}$ (Eq. 8). In particular, in order to minimize a doubly excited configuration in a molecular orbital basis, we require matrix elements of the form $f^{xc}_{ih,jh}$, $f^{xc}_{ih,al}$, and $f^{xc}_{al,bl}$. Unfortunately, within current computational codes (e.g. Q-Chem[59]), such matrix elements are not readily available and we have currently implemented a painful (and slow) approach towards calculating these $\sim N^2$ matrix elements. Future work will necessarily need to construct these matrix elements in a timely and efficient fashion in order for the TD-DFT-1D approach to be fast and competitive. This project is now ongoing.

5 Conclusion

We have shown that Newton-Raphson optimization is stable as far as finding the optimal doubly excited state for the CIS-1D and the TDDFT-1D method, and these configuration interaction Hamiltonian can successfully recover electronic potential energy surfaces states corresponding to bond making/breaking processes. Furthermore, one can use such approaches to produce meaningful diabatic states through adiabatic-to-diabatic transformations (e.g. the Boys diabatization method). We have shown that in situations where DFT/TD-DFT recovers an S_0/S_1 crossing incorrectly, TDDFT-1D method can recover qualitatively correct

energy curves. Finally, once the necessary matrix elements of f^{xc} are computed efficiently, the present method should be applicable to quite large molecules and act as an alternative to spin-flip methods.[29,60] Lastly, if one can successfully apply the techniques of Ref. 61 for CIS-1D analytical derivatives[62] to the TDDFT-1D method, simulating nonadiabatic chemical dynamics[63] within such an ansatz should be in the near horizon.

Acknowledgement

A   Dipole moments of CIS-1D/TDDFT-1D states

Here, we provide the relevant equations for obtaining dipole moments in a CIS-1D calculation. A CIS-1D state is a linear combination of its basis states:

$$|\psi_{CIS-1D}\rangle = c_0 |\phi_0\rangle + \sum_{ia} \frac{1}{\sqrt{2}} c_i^a (|\phi_i^a\rangle + |\phi_{\bar{i}}^{\bar{a}}\rangle) + c_d \left|\phi_{h\bar{h}}^{l\bar{l}}\right\rangle. \tag{9}$$

Note that the ground state HF wave function is restricted, and the CIS states are singlets. The dipole moment between two CIS-1D states is then given by

$$\begin{aligned}
\langle\psi^I|X|\psi^J\rangle = {} & c_o^I c_0^J X_0 + \sum_{ia} \sqrt{2}(c_o^I c_i^{aJ} + c_o^J c_i^{aI}) X_{ia} \\
& + \sum_{ia} c_i^{aI} c_i^{aJ} X_0 + \sum_{iab} c_i^{aI} c_i^{bJ} X_{ab} - \sum_{ija} c_i^{aI} c_j^{aJ} X_{ij} \\
& + \sum_{ia} \sqrt{2}(c_h^{lI} c_d^J + c_h^{lJ} c_d^I) X_{hl} + c_d^I c_d^J (X_0 + 2X_{ll} - 2X_{hh}). \tag{10}
\end{aligned}$$

Here X_0 is the ground state dipole moment, and X_{pq} are the elements of the dipole moment matrix.

References

(1) Mok, D. K.; Neumann, R.; Handy, N. C. Dynamical and nondynamical correlation. *The Journal of Physical Chemistry* **1996**, *100*, 6225–6230.

(2) Benavides-Riveros, C. L.; Lathiotakis, N. N.; Marques, M. A. Towards a formal definition of static and dynamic electronic correlations. *Physical Chemistry Chemical Physics* **2017**, *19*, 12655–12664.

(3) Via-Nadal, M.; Rodríguez-Mayorga, M.; Ramos-Cordoba, E.; Matito, E. Singling out dynamic and nondynamic correlation. *The journal of physical chemistry letters* **2019**, *10*, 4032–4037.

(4) Møller, C.; Plesset, M. S. Note on an approximation treatment for many-electron systems. *Physical review* **1934**, *46*, 618.

(5) Jones, R. O. Density functional theory: Its origins, rise to prominence, and future. *Rev. Mod. Phys.* **2015**, *87*, 897–923.

(6) Mardirossian, N.; Head-Gordon, M. Thirty years of density functional theory in computational chemistry: an overview and extensive assessment of 200 density functionals. *Molecular Physics* **2017**, *115*, 2315–2372.

(7) Verma, P.; Truhlar, D. G. Status and challenges of density functional theory. *Trends in Chemistry* **2020**, *2*, 302–318.

(8) Peverati, R. Fitting elephants in the density functionals zoo: Statistical criteria for the evaluation of density functional theory methods as a suitable replacement for counting parameters. *International Journal of Quantum Chemistry* **2021**, *121*, e26379.

(9) Yarkony, D. R. Diabolical conical intersections. *Rev. Mod. Phys.* **1996**, *68*, 985–1013.

(10) Yarkony, D. R. Conical intersections: The new conventional wisdom. *The Journal of Physical Chemistry A* **2001**, *105*, 6277–6293.

(11) Worth, G. A.; Cederbaum, L. S. Beyond Born-Oppenheimer: molecular dynamics through a conical intersection. *Annu. Rev. Phys. Chem.* **2004**, *55*, 127–158.

(12) Nunn, A.; Minns, R.; Spesyvtsev, R.; Bearpark, M.; Robb, M.; Fielding, H. Ultrafast dynamics through conical intersections and intramolecular vibrational energy redistribution in styrene. *Physical Chemistry Chemical Physics* **2010**, *12*, 15751–15759.

(13) Yarkony, D. R. S1- S0 Internal Conversion in Ketene. 1. The Role of Conical Intersections. *The Journal of Physical Chemistry A* **1999**, *103*, 6658–6668.

(14) Fuß, W.; Pushpa, K. K.; Rettig, W.; Schmid, W. E.; Trushin, S. A. Ultrafast charge transfer via a conical intersection in dimethylaminobenzonitrile. *Photochemical & Photobiological Sciences* **2002**, *1*, 255–262.

(15) Tishchenko, O.; Li, R.; Truhlar, D. G. Metal-organic charge transfer can produce biradical states and is mediated by conical intersections. *Proceedings of the National Academy of Sciences* **2010**, *107*, 19139–19145.

(16) Levine, B. G.; Martínez, T. J. Isomerization through conical intersections. *Annu. Rev. Phys. Chem.* **2007**, *58*, 613–634.

(17) Levine, B. G.; Ko, C.; Quenneville, J.; MartÍnez, T. J. Conical intersections and double excitations in time-dependent density functional theory. *Molecular Physics* **2006**, *104*, 1039–1051.

(18) Gagliardi, L.; Truhlar, D. G.; Li Manni, G.; Carlson, R. K.; Hoyer, C. E.; Bao, J. L. Multiconfiguration Pair-Density Functional Theory: A New Way To Treat Strongly Correlated Systems. *Accounts of Chemical Research* **2017**, *50*, 66–73.

(19) Sand, A. M.; Hoyer, C. E.; Truhlar, D. G.; Gagliardi, L. State-interaction pair-density functional theory. *The Journal of chemical physics* **2018**, *149*, 024106.

(20) Grimme, S.; Waletzke, M. A combination of Kohn–Sham density functional theory and multi-reference configuration interaction methods. *The Journal of Chemical Physics* **1999**, *111*, 5645–5655.

(21) Marian, C. M.; Heil, A.; Kleinschmidt, M. The DFT/MRCI method. *WIREs Computational Molecular Science* **2019**, *9*, e1394.

(22) Yang, Y.; Shen, L.; Zhang, D.; Yang, W. Conical Intersections from Particle–Particle Random Phase and Tamm–Dancoff Approximations. *The Journal of Physical Chemistry Letters* **2016**, *7*, 2407–2411.

(23) Kaduk, B.; Van Voorhis, T. Communication: Conical intersections using constrained density functional theory–configuration interaction. *The Journal of Chemical Physics* **2010**, *133*, 61102.

(24) Kowalczyk, T.; Tsuchimochi, T.; Chen, P.-T.; Top, L.; Van Voorhis, T. Excitation energies and Stokes shifts from a restricted open-shell Kohn-Sham approach. *The Journal of Chemical Physics* **2013**, *138*, 164101.

(25) Evangelista, F. A.; Shushkov, P.; Tully, J. C. Orthogonality Constrained Density Functional Theory for Electronic Excited States. *The Journal of Physical Chemistry A* **2013**, *117*, 7378–7392.

(26) Shu, Y.; Parker, K. A.; Truhlar, D. G. Dual-functional Tamm–Dancoff approximation: a convenient density functional method that correctly describes S1/S0 conical intersections. *The journal of physical chemistry letters* **2017**, *8*, 2107–2112.

(27) Li, S. L.; Marenich, A. V.; Xu, X.; Truhlar, D. G. Configuration interaction-corrected Tamm–Dancoff approximation: A time-dependent density functional method with the correct dimensionality of conical intersections. *The journal of physical chemistry letters* **2014**, *5*, 322–328.

(28) Shao, Y.; Head-Gordon, M.; Krylov, A. I. The spin–flip approach within time-dependent density functional theory: Theory and applications to diradicals. *The Journal of Chemical Physics* **2003**, *118*, 4807–4818.

(29) Casanova, D.; Krylov, A. I. Spin-flip methods in quantum chemistry. *Physical Chemistry Chemical Physics* **2020**, *22*, 4326–4342.

(30) Zhang, X.; Herbert, J. M. Excited-State Deactivation Pathways in Uracil versus Hydrated Uracil: Solvatochromatic Shift in the 1 n π* State is the Key. *The Journal of Physical Chemistry B* **2014**, *118*, 7806–7817.

(31) Winslow, M.; Cross, W. B.; Robinson, D. Comparison of Spin-Flip TDDFT-Based Conical Intersection Approaches with XMS-CASPT2. *Journal of chemical theory and computation* **2020**, *16*, 3253–3263.

(32) Kaduk, B.; Kowalczyk, T.; Van Voorhis, T. Constrained density functional theory. *Chemical reviews* **2012**, *112*, 321–370.

(33) Kaduk, B.; Van Voorhis, T. Communication: Conical intersections using constrained density functional theory–configuration interaction. 2010.

(34) Mei, Y.; Yang, W. Excited-State Potential Energy Surfaces, Conical Intersections, and Analytical Gradients from Ground-State Density Functional Theory. *The Journal of Physical Chemistry Letters* **2019**, *10*, 2538–2545.

(35) Qu, Z.; Ma, Y. Variational Multistate Density Functional Theory for a Balanced Treatment of Static and Dynamic Correlations. *Journal of chemical theory and computation* **2020**, *16*, 4912–4922.

(36) Gräfenstein, J.; Cremer *, D. Development of a CAS-DFT method covering non-dynamical and dynamical electron correlation in a balanced way. *Molecular Physics* **2005**, *103*, 279–308.

(37) Bauschlicher, C. W.; Langhoff, S. R. Full configuration-interaction study of the ionic–neutral curve crossing in LiF. *The Journal of Chemical Physics* **1988**, *89*, 4246–4254.

(38) Zaitsevskii, A.; Malrieu, J.-P. The discontinuities of state-average MCSCF potential surfaces. *Chemical Physics Letters* **1994**, *228*, 458–462.

(39) Sanchez de Meras, A.; Lepetit, M.-B.; Malrieu, J.-P. Discontinuity of valence CASSCF wave functions around weakly avoided crossing between valence configurations. *Chemical Physics Letters* **1990**, *172*, 163–168.

(40) Teh, H.-H.; Subotnik, J. E. The Simplest Possible Approach for Simulating S0–S1 Conical Intersections with DFT/TDDFT: Adding One Doubly Excited Configuration. *The Journal of Physical Chemistry Letters* **2019**, *10*, 3426–3432.

(41) Maitra, N. T.; Zhang, F.; Cave, R. J.; Burke, K. Double excitations within time-dependent density functional theory linear response. *The Journal of Chemical Physics* **2004**, *120*, 5932–5937.

(42) Fetter, A.; Walecka, J. Quantum Theory of Many Particle Systems, Chap. 13. 1971.

(43) Hirata, S.; Head-Gordon, M. Time-dependent density functional theory within the Tamm–Dancoff approximation. *Chemical Physics Letters* **1999**, *314*, 291–299.

(44) Bixon, M.; Jortner, J.; Verhoeven, J. W. Lifetimes for radiative charge recombination in donor-acceptor molecules. *Journal of the American Chemical Society* **1994**, *116*, 7349–7355.

(45) Liu, X.; Subotnik, J. E. The variationally orbital-adapted configuration interaction singles (VOA-CIS) approach to electronically excited states. *Journal of chemical theory and computation* **2014**, *10*, 1004–1020.

(46) Subotnik, J. E.; Yeganeh, S.; Cave, R. J.; Ratner, M. A. Constructing diabatic states from adiabatic states: Extending generalized Mulliken–Hush to multiple charge centers with Boys localization. *The Journal of chemical physics* **2008**, *129*, 244101.

(47) Ben-Nun, M.; Martınez, T. J. Photodynamics of ethylene: Ab initio studies of conical intersections. *Chemical Physics* **2000**, *259*, 237–248.

(48) Zhang, F.; Wu, D.; Xu, Y.; Feng, X. Thiophene-based conjugated oligomers for organic solar cells. *Journal of Materials Chemistry* **2011**, *21*, 17590–17600.

(49) Rupert, B. L.; Mitchell, W. J.; Ferguson, A. J.; Köse, M. E.; Rance, W. L.; Rumbles, G.; Ginley, D. S.; Shaheen, S. E.; Kopidakis, N. Low-bandgap thiophene dendrimers for improved light harvesting. *Journal of Materials Chemistry* **2009**, *19*, 5311–5324.

(50) Mazzeo, M.; Pisignano, D.; Favaretto, L.; Barbarella, G.; Cingolani, R.; Gigli, G. Bright oligothiophene-based light emitting diodes. *Synthetic metals* **2003**, *139*, 671–673.

(51) Kölle, P.; Schnappinger, T.; de Vivie-Riedle, R. Deactivation pathways of thiophene and oligothiophenes: internal conversion versus intersystem crossing. *Physical Chemistry Chemical Physics* **2016**, *18*, 7903–7915.

(52) Belletete, M.; Leclerc, M.; Durocher, G. Potentialities of Semiempirical Calculations (AMPAC and INDO/S) in Determining the Conformation and Electronic Properties of 2, 2'-Bithiophene: A New Joint Experimental and Theoretical Approach. *The Journal of Physical Chemistry* **1994**, *98*, 9450–9456.

(53) Dutoi, A. D.; Head-Gordon, M. Self-interaction error of local density functionals for alkali–halide dissociation. *Chemical physics letters* **2006**, *422*, 230–233.

(54) Zhang, Y.; Yang, W. A challenge for density functionals: Self-interaction error increases for systems with a noninteger number of electrons. *The Journal of Chemical Physics* **1998**, *109*, 2604–2608.

(55) Chai, J.-D.; Head-Gordon, M. Long-range corrected hybrid density functionals with damped atom–atom dispersion corrections. *Phys. Chem. Chem. Phys.* **2008**, *10*, 6615–6620.

(56) Fdez. Galván, I. et al. OpenMolcas: From Source Code to Insight. *Journal of Chemical Theory and Computation* **2019**, *15*, 5925–5964, PMID: 31509407.

(57) Varandas, A. Accurate ab initio potential energy curves for the classic Li–F ionic-covalent interaction by extrapolation to the complete basis set limit and modeling of the radial nonadiabatic coupling. *The Journal of chemical physics* **2009**, *131*, 124128.

(58) Bulewicz, E.; Phillips, L.; Sugden, T. Determination of dissociation constants and heats of formation of simple molecules by flame photometry. Part 8.—Stabilities of the gaseous diatomic halides of certain metals. *Transactions of the Faraday Society* **1961**, *57*, 921–931.

(59) Shao, Y. et al. Advances in molecular quantum chemistry contained in the Q-Chem 4 program package. *Molecular Physics* **2015**, *113*, 184–215.

(60) Zhang, X.; Herbert, J. M. Spin-flip, tensor equation-of-motion configuration interaction with a density-functional correction: A spin-complete method for exploring excited-state potential energy surfaces. *The Journal of chemical physics* **2015**, *143*, 234107.

(61) Teh, H.-H.; Subotnik, J. E. Analytic gradients and derivative couplings for configuration interaction with all single excitations and one double excitation—En route to nonadiabatic dynamics. *The Journal of Chemical Physics* **2020**, *153*, 184106.

(62) Send, R.; Furche, F. First-order nonadiabatic couplings from time-dependent hybrid density functional response theory: Consistent formalism, implementation, and performance. *The Journal of chemical physics* **2010**, *132*, 044107.

(63) Salazar, E.; Faraji, S. Theoretical study of cyclohexadiene/hexatriene photochemical interconversion using spin-Flip time-Dependent density functional theory. *Molecular Physics* **2020**, *118*, e1764120.

Graphical TOC Entry